Contents lists available at ScienceDirect

Nuclear Instruments and Methods in Physics Research B

PIXE identification of the provenance of ferruginous rocks used by Neanderthals

François Mathis [a,*], Pierre Bodu [b], Olivier Dubreuil [c], Hélène Salomon [d]

[a] Centre Européen d'Archéométrie, University of Liège, Belgium
[b] ARSCAN, UMR4071 CNRS, MAE, Nanterre, France
[c] Centre Spatial de Liège, Liège, Belgium
[d] Service de Préhistoire, University of Liège, Liège, Belgium

ABSTRACT

Les Bossats, near Ormesson, France, is a newly discovered late Mousterian open air site dated to around 47,000 years ago by thermoluminescence. The archaeological level, fossilized by loess, revealed a rich industry based on the discoid mode, associated with numerous fragments of red and yellow iron oxide-rich rocks showing clear traces of powder production (abrasion, striation, scraping), which are exceptional remains for this remote period. Archeological material and geological samples from the close environment were studied by PIXE and by petrographical observations made on thin sections. The geological sources were identified by means of PIXE analyses on two IBA facilities: AGLAE (2 MV tandem) at the C2RMF in Paris and the cyclotron of the IPNAS (University of Liège). We paid particular attention to the comparison of results obtained on both installations by using the same set of geological standards and by a fine evaluation of the limit of detection relative to each trace elements of interest for both experimental set ups. The elemental fingerprint of one geological source of iron-rich concretions corresponds clearly with the archaeological collection. At least, this investigation demonstrates that the colouring materials were minutely selected in the close neighbouring of the site by the Neanderthals.

© 2014 Elsevier B.V. All rights reserved.

1. Introduction

1.1. Fingerprinting iron oxide rich-rocks from the Palaeolithic

Colouring materials used by the hunter-gatherers of the Palaeolithic are commonly refereed as "ochre", although they are iron oxide-rich rocks. In the past few years, papers focused on the identification of geochemical fingerprints of archaeological and geological colouring rocks by XRF (X-ray Fluorescence) [1], ICP-MS (Inductively Coupled Plasma Mass Spectrometry) [2–4], neutron activation analysis [5–8] and PIXE [9–15]. Except for PIXE, sample preparation is required.

In this paper, we determined, without any preliminary preparation, the chemical fingerprint of the archaeological ferruginous stones and geological references extracted in the area surrounding the Mousterian site, by comparing the analytical results obtained with AGLAE and the cyclotron in Liège.

1.2. Archaeological context

"Les Bossats", in Ormesson is a Late Mousterian settlement, located in France, 70 km south of Paris, dated around 47,000 B.P.

[16], displaying a rich flaked industry associated with many fragments and smoothed, faceted, grooved, striated blocks of iron oxide-rich stones (Fig. 1), which are relatively uncommon artefacts for Middle Palaeolithic contexts [17–26].

2. Material and methods

2.1. Geological and archaeological ferruginous rocks

Within the archaeological collection, a single type of raw material was identified, made of a succession of different layers, red, grey and yellow. These morphological and mineral characteristics are typical of ferruginous concretions formed in continental detrital layers under tropical climatic conditions [27–29]. All the colouring artefacts present the same characteristics.

Archaeological settlement is situated in a geological environment dominated by Sparnatian detrital formation and Stampian sandy horizon. Both contexts provide ferruginous rocks manly sandstones and concretion that were sampled for this study.

The Stampian sand contents punctually ferruginous concretions. "Les Crottes de Fer" in Larchant, some 5 km to the north-west of the Mousterian camp-site provided geological references (Fig. 2).

The Sparnacian detrital continental formation[30,31] provides ferruginous concretions and ferruginous sandstones nowadays

* Corresponding author. Tel.: +32 43663681.
  E-mail address: francois.mathis@ulg.ac.be (F. Mathis).

Fig. 1. Ferruginous stones showing traces of abrasion by rubbing and scraping. All of them were removed from level 4, a late Mousterian camp site.

situated around 40 km east from the site, in the area of Pont-sur-Yonne and Villemer.

In order to discriminate the raw ferruginous concretion, major and trace elements were measured by PIXE, for each geological formation and for archaeological remains to compare their geochemical fingerprints.

Therefore, major and trace elemental content was quantified for:

- Six geological samples from the Stampian.
- 12 Geological samples from the Sparnacian (TRG11 and TRG24 are ferruginous sandstones).
- 11 Ferruginous concretions collected in the Mousterian level 4.

Two to four measures were made for each object taking into account the different layers (haematite-rich and goethite-rich). Furthermore, the concretions showing wear traces were preferentially analysed, as they are the most relevant material for investigating procurement strategies, in particular the choices of materials.

2.2. PIXE experimental set ups: AGLAE (C2RMF, Paris) and Cyclotron (IPNAS, Liège)

For practical reasons, PIXE experiments were conducted in two different places: at the AGLAE (Accélérateur Grand Louvre d'Analyse Elémentaire) facility based in Paris, France and at the PIXE facility of the University of Liège, Belgium. Therefore, ensuring comparable working conditions and results was one of the key issues and special care was taken to it during both experimental work and data treatment.

AGLAE is a 2 MV tandem accelerator as the Belgium facility is an Azimutal Varying Field cyclotron, both were used to deliver a 3 MeV proton extracted beam. The beam size in Liège is about 1 mm diameter, at AGLAE the beam size is about 50 µm diameter, to ensure that the volume analysed is almost equivalent and because the samples are highly heterogeneous, the beam is scanned over a 1 mm^2 area. In both cases, beams are extracted through a 100 nm thick Si_3N_4 window and Helium is blown between the window and the sample to avoid beam straggling.
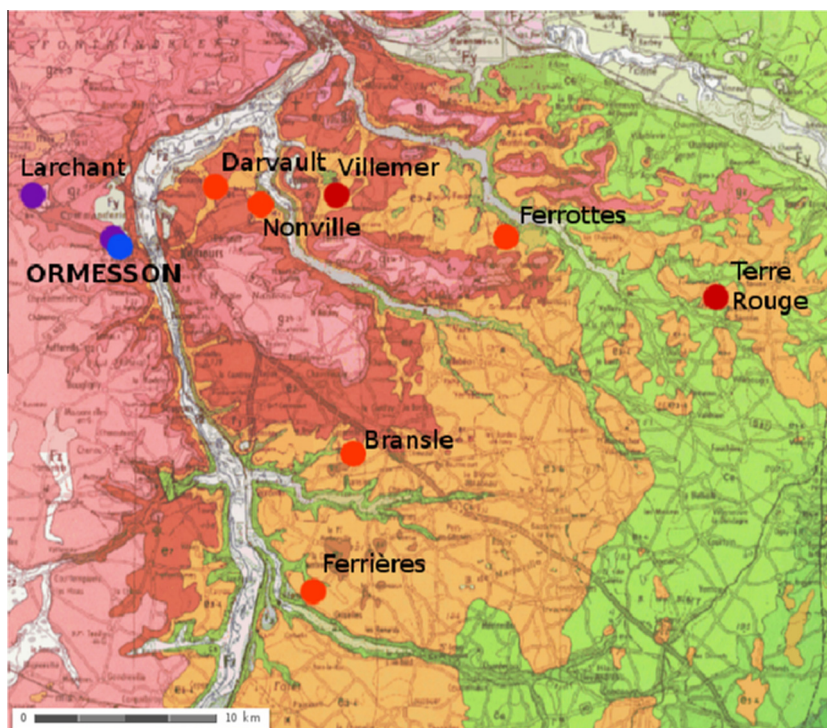

Fig. 2. Geological maps with mention of our surveys. The archaeological site is located with a blue dot. The Stampian is pink and the sample spots are violet. The Sparnacian is coloured with orange, the orange spots indicate mention of ancient iron ore exploit. (For interpretation of the references to color in this figure legend, the reader is referred to the web version of this article.)

X-ray spectra are recorded by two detectors oriented at 45° to the beam direction. One is devoted to the low energy X-rays coming from the light elements of the matrix of our samples (Si, Al, Ca, Fe). The detector is the same in both places, a Si(Li) detector equipped with an ultra-thin polymer window (AP3.3 from Moxtek®), Helium is blown between the sample and the detector to avoid low energy X-ray absorption. The other detector is devoted to the detection of high energy X-rays (6–35 keV) emitted by trace elements and equipped with a selective filter in order to reduce signal and pile-up coming from major elements. In AGLAE this detector is a 50 mm^2 Si(Li) [32] detector with a Beryllium window, the chosen filter is a 20 µm thick chromium filter (deposited on 150 µm polymer film) to absorb Fe X-rays and an additional 50 µm thick aluminium filter was used to reduce the secondary X-rays coming from the Cr filter. At Liège the trace detector is an Ultra-LEGe detector from Canberra with a 0.3 mm thick Beryllium window [33]. The chosen filter was a 10 µm thick chromium filter (mounted on 150 µm polymer film). All the characteristics of the two set-ups are summarized in Table 1.

PIXE spectra were collected between 10 and 15 min with a current of about 5 nA at AGLAE and 7 nA in Liège for a total fluence almost equivalent in both case of about 4 µC.

To compare the results we analysed the same standards (DR-N, MA-N, BE-N, UB-N which are geological standards from CRPG) and one archaeological sample (5 points analysed) on both devices to compare data from both laboratories and these measures confirmed a very satisfactory reproducibility. The use of selective filters gives access to detection limits less than 10 ppm to around 100 ppm according to the elements. They are detailed in Table 2. Examples of spectra acquired in both places on the same sample are presented in Fig. 3. The spectra of the matrix are almost equivalent as the spectra of the trace elements are more detailed in AGLAE with a higher total number of count which can be explained by a better geometry optimization and a higher solid angle, which explains the difference we observe on the LOD of traces elements between both set-ups.

This difference in the limit of detection between both set-ups was a crucial point in the choice of relevant trace elements for determining the provenance of iron ores.

Elemental concentrations have been extracted by using GUPIX-WIN [34]. The elemental concentration of the matrix were calculated by normalizing to 100% in oxide mode while the traces elements were calculated by normalizing the iron value to the value found in the matrix calculation. The automatized treatment was performed by using TRAUPIXE [32] which run automatically GUPIX-WIN for the calculation of matrix and traces elements for each point and extract the concentration, errors and LOD and other parameters from the GUPIXWIN output files and class them in a table.

3. Provenance of colouring materials

To determine automatically the detection of trace elements while taking into account the differences in the LOD between the set-ups we compare the elemental concentration minus its error

Table 1
Characteristic of the two set-ups used.

	Beam	Beam size	Scanned area	Detector low energy	Filter	Detector High Energy	Filter	Current	Time of Aquisition	Total Fluence
AGLAE	P 3 MeV	50 µm	1 * 1 mm^2	Si(Li) 10 mm^2	Ultra thin window + He	Si(Li) 50 mm^2	Be window Cr 20 µm Al 50 µm	5 nA	10–15 min	3–4 µC
Liege	P 3 MeV	1 mm		Si(Li) 10 mm^2	Ultra thin window + He	Ultra-LEGe 50 mm^2	Be window Cr 10 µm	7 nA	10 min	4 µC

Table 2
PIXE limit of detection (LOD) in ppm for elements heavier than iron for the two set-ups.

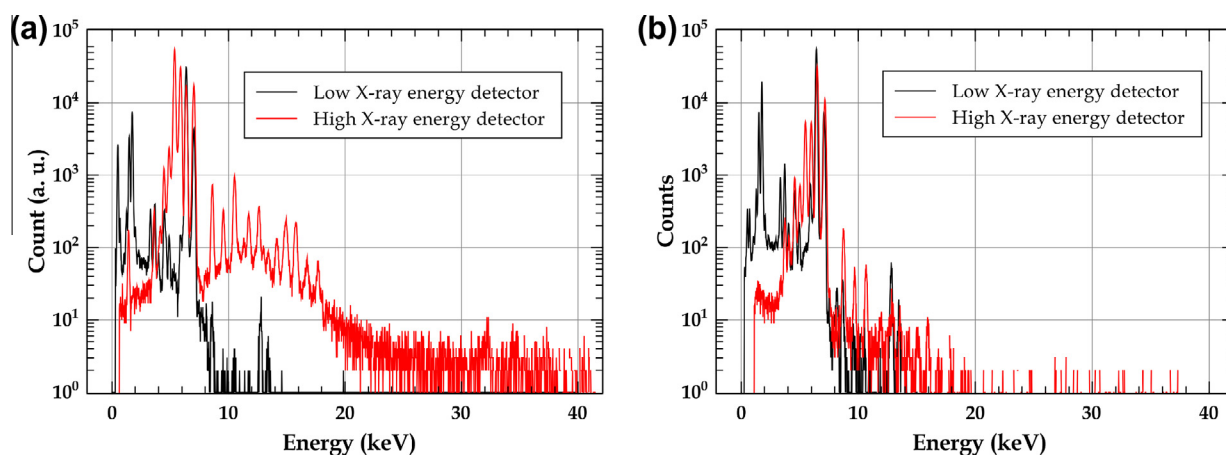|	Ni	Cu	Zn	Ga	As	Rb	Sr	Y	Zr	Nb	Mo	Ag	Sn	Sb	Ba	W	Pb	Bi
AGLAE	22	8	3	4	8	2	2	3	3	4	3	5	4	9	17	43	59	16
Liège	36	12	10	10	15	20	10	17	18	16	26	37	46	40	330	63	87	27

Fig. 3. PIXE spectra for major (black) and trace (red) elements for the archaeological sample OR10E40–10. Comparison between AGLAE (left) and Liège (right). (a) AGLAE high energy spectrum shows a large panel of trace elements emerging from the background. (b) Liège high energy spectrum shows less trace elements. (For interpretation of the references to color in this figure legend, the reader is referred to the web version of this article.)
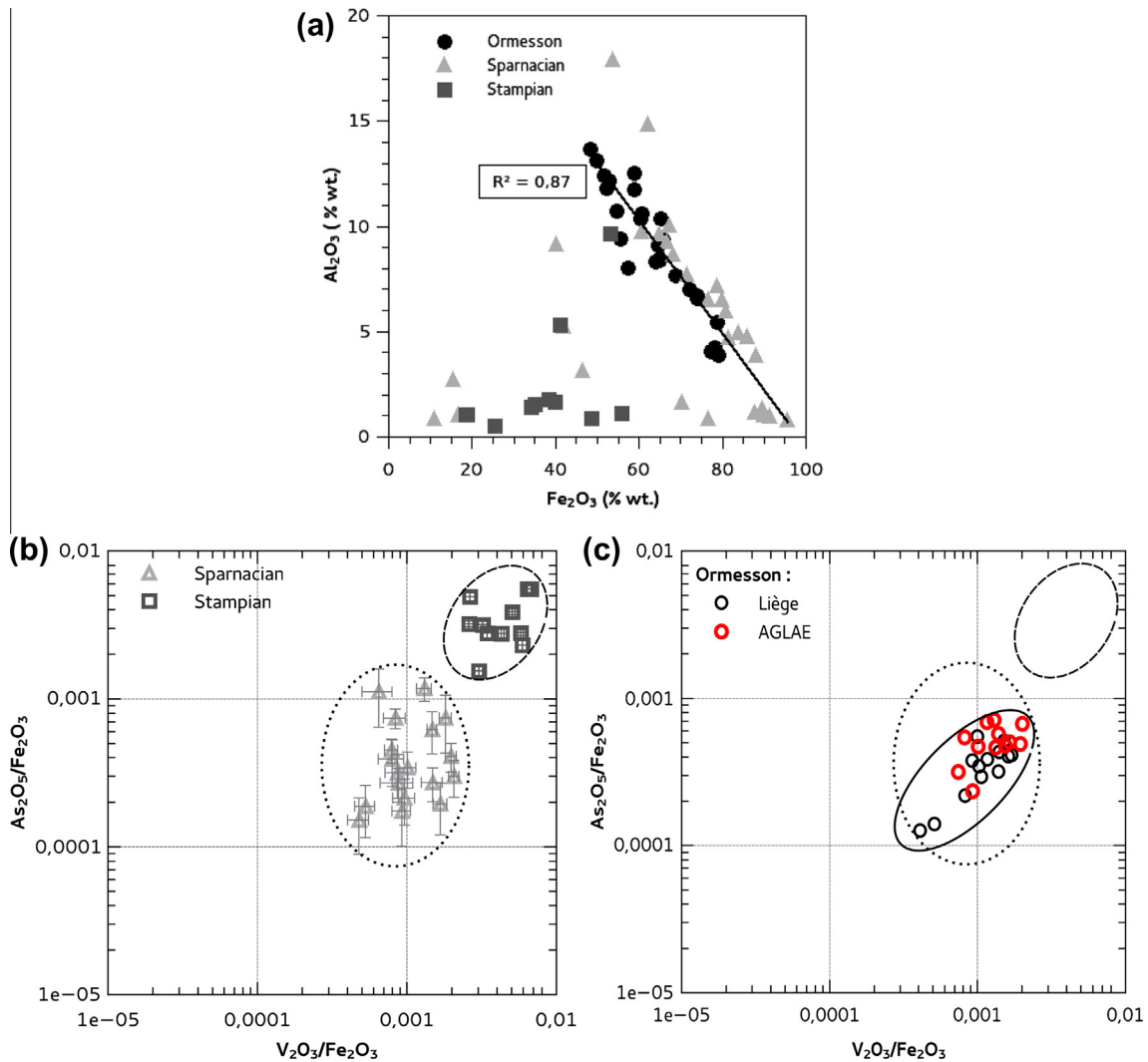
Fig. 4. (a) The anti-correlation of Al2O3 and Fe2O3 indicate the contribution of weathering of the ferruginous crust. It affects the archaeological collection and the ferruginous concretion from the Sparnacian. The Sparnacian ferruginous sandstones and the Stampian concretions are not following the same tendency. (b) As_2O_5/Fe_2O_3 concentration as a function of V_2O_3/Fe_2O_3 concentration shows a clear discrimination of both geological formations with a confidence ellipse of 1 sigma (1 fit) and (c) plot of the archaeological samples measured in IPNAS (black) and in AGLAE (red) with a 1 sigma confidence ellipse. (For interpretation of the references to color in this figure legend, the reader is referred to the web version of this article.)

(Fit Error parameter of Gupix) to the Limit of Detection and we keep only the values of concentration that passed this test.

The group of provenance are graphically obtained (Fig. 4a) by plotting an ellipsoid covering all the points of the same provenance with their error bars calculated using the fit error parameter of GUPIXWIN, which are reported in Table 3.

Trace element composition provides chemical markers which are used to establish distinctions between different types of ferruginous rocks, using Pearson test and bivariate plots of iron and trace elements for each category of material following the methodology described in previous studies [5,6,9,10]. All the elements related to any kind of possible contamination, such as Cl, S, Ca, Ba, Mn, have been rejected after verification with analysis and observations using SEM-EDX.

Concerning the major elements, a first discrimination between the two geological sources can be evidenced by looking at weathering contribution (Al_2O_3, TiO_2) versus Iron oxide content.

The Stampian geological samples present lower iron contents than the Sparnacians. This latest group is divided into two populations corresponding to both types of rock (concretions and ferruginous sandstone) present in this formation. The Sparnacian concretions present a clear anti correlation between Al_2O_3 or TiO_2 and Fe_2O_3 (Fig. 4a) characteristic of the weathering processes of this type of rock as TiO_2 replaces SiO_2 in the phyllosilicates during weathering. Archaeological materials seem to follow the same behaviour contrary to the Stampian concretions and the Sparnacian sandstones.

Looking at the trace elements we determined that Vanadium (V) and arsenic (As) concentrations are particularly dependant on iron (Fe) concentrations in the archaeological remains and in Sparnacian concretions and sandstones (Table 3). To the contrary, Stampian samples which present higher content in these elements. Therefore, these elements allow the discrimination of two coherent chemical groups of geological sources whatever the type of rocks (Fig. 4b).

This analysis evidences a chemical match between the ferruginous concretions and sandstones from the Sparnacian and the Mousterian concretions. Consequently according to these results, the Stampian concretions can be ruled out as possible sources of colouring materials (Fig. 4c).

Furthermore, as the ferruginous sandstones are not represented within the archaeological collection, we can assume that only ferruginous concretions were looked for and selected. The supply in ferruginous concretions seems then likely to be local, at least 5 km away from the camp site, on the other bank of the Loing river.

In addition, one has to note that both discriminating elements are in sufficient contents to be measured in both detection setups to allow intercomparison of results.

4. Conclusions

Although the Stampian concretions were available in the nearest area around the settlement, they were not selected. The selection of raw ferruginous material therefore indicates that, in order to transform the raw matrix, some visual and mechanical properties were privileged such as the high iron oxide content and few quartz, as well as the little hardness of haematite layers and their fine crystallisation. All these characteristics seem to have been favourable for their further transformations, which left use wear traces consisting in facets, polished surfaces, grooves and negatives of flakes.

The archaeological collection reveals a systematic sourcing in the same geological layer, whose outcrops were probably situated at least 5 km from the camp-site at that time. The Mousterians therefore neglected the local ferruginous concretions, most probably available on the site itself (as documented by the excavation in level 5 during season 2012) or in the neighbouring sandy chaos from the Stampian. They privileged the use of ferruginous concretions, quite exclusively composed of iron oxides (haematite) and hydroxides (goethite), which were selected minutely in the outcrops. We can assume that the collect of ferruginous materials was not opportunistic because of the choice of raw material made by the Neanderthals.

Evidencing the geochemical fingerprint of raw ferruginous rocks requires to analyse many samples. This situation force to perform analysis during several campaigns and possibly with different devices. We demonstrated that the results are reliable, as long as control of many experimental parameters is ensured.

Appendix A. Supplementary data

Supplementary data associated with this article can be found, in the online version, at http://dx.doi.org/10.1016/j.nimb.2013.11.028.

References

[1] M. Gil, M.L. Carvalho, A. Seruya, A.E. Candeias, J. Mirão, I. Queralt, Nuclear instruments and methods in Physics research section A: accelerators, Spectrom. Detect. Assoc. Equip. 580 (2007) 728.
[2] R.L. Green, R.J. Watling, J. Forensic Sci. 52 (2007) 851.
[3] E. Iriarte, A. Foyo, M.A. Sánchez, C. Tomillo, J. Setién, Archaeometry 51 (2009) 231.
[4] P. Jezequel, G. Wille, C. Beny, F. Delorme, V. Jean-Prost, R. Cottier, J. Breton, F. Dure, J. Despriee, J. Archaeol. Sci. 38 (2011) 1165.
[5] B.S. Eiselt, R.S. Popelka-Filcoff, J.A. Darling, M.D. Glascock, J. Archaeol. Sci. 38 (2011) 3019.
[6] R.S. Popelka-Filcoff, C.E. Lenehan, M.D. Glascock, J.W. Bennett, A. Stopic, J.S. Quinton, A. Pring, K. Walshe, J. Radioanal. Nucl. Chem. 291 (2012) 19.
[7] R.S. Popelka-Filcoff, E.J. Miksa, J.D. Robertson, M.D. Glascock, H. Wallace, J. Archaeol. Sci. 35 (2008) 752.
[8] R.S. Popelka-Filcoff, J.D. Robertson, M.D. Glascock, C. Descantes, J. Radioanal. Nucl. Chem. 272 (2007) 17.
[9] L. Beck, M. Lebon, L. Pichon, L. Menu, R. Chiotti, R. Nespoulet, P. Paillet, X-Ray Spectrom. 40 (2011) 219.
[10] L. Beck, H. Salomon, S. Lahlil, M. Lebon, G.P. Odin, Y. Coquinot, L. Pichon, Nucl. Instru. Methods Phys. Res. Sect. B: Beam Interact. Mater. Atoms 273 (2012) 173.
[11] D.C. Creagh, M.E. Kubik, M. Sterns, Nucl. Instrum. Methods Phys. Res., Sect. A: Accel. Spect. Detect. Assoc. Equip. 580 (2007) 721.
[12] B. David, E. Clayton, A. Watchman, Austr. Archaeol. (1993) 50.
[13] J.M. Erlandson, J.D. Robertson, C. Descantes, Am. Antiq. 64 (1999) 517.
[14] P. Nel, P.A. Lynch, J.S. Laird, H.M. Casey, L.J. Goodall, C.G. Ryan, R.J. Sloggett, Nucl. Instrum. Methods Phys. Res. Sect. A: Accel. Spectro., Detect. Assoc. Equip. 619 (2010) 306.
[15] M. Sánchez del Río, P. Martinetto, C. Solís, C. Reyes-Valerio, Nucl. Instrum. Methods Phys. Res. Sect. B: Beam Interac. Mater. Atoms 249 (2006) 628.
[16] P. Bodu, H. Salomon, J. Lacarrière, M. Leroyer, M. Dessoles, Quater. Int., 2013 (in press) (Available online 28 October 2013).
[17] C.S. Henshilwood et al., Science 295 (2002) 1278.
[18] C.W. Marean et al., Nature 449 (2007) 905.
[19] P. Van Peer, R. Fullagar, S. Stokes, R.M. Bailey, J. Moeyersons, F. Steenhoudt, A. Geerts, T. Vanderbeken, M. De Dapper, F. Geus, J. Hum. Evol. 45 (2003) 187.
[20] L. Wadley, T. Hodgskiss, M. Grant, Proc. Nat. Acad. Sci. 106 (2009) 9590.
[21] I. Watts, South Afr. Archaeol. Bullet. 57 (2002) 1.
[22] I. Watts, J. Hum. Evol. 59 (2010) 392.
[23] F. d'Errico, H. Salomon, C. Vignaud, C. Stringer, J. Archaeol. Sci. 37 (2010) 3099.
[24] E. Hovers, S. Ilani, O. BarYosef, B. Vandermeersch, Curr. Anthropol. 44 (2003) 491.
[25] H. Salomon, C. Vignaud, Y. Coquinot, L. Beck, C. Stringer, D. Strivay, F. D'Errico, Archaeometry 54 (2012) 698.
[26] J. Zilhão et al., Proc. Nat. Acad. Sci. 107 (2010) 1023.
[27] U. Schwertmann, R.W. Fitzpatrick, Catena Suppl. 21 (1992) 7.
[28] A. Seilacher, Sed. Geol. 143 (2001) 41.
[29] P. Mozley, Diagenetic Structures, in: G. Middleton (Ed.), Encyclopedia of Sedimentsand Sedimentary Rocks, Kluwer Academic Press, Dordrecht, 2003, p. 219.
[30] R. Bouiller, M. Turland, P.-L. Vincent, Carte Géologique de la France n°295, 1/50000ème, Montereau-Faut-Yonne. in: BRGM (Ed.), Orléans, 1973.
[31] M. Thiry, Sédimentation continentale et altérations associées: calcitisations, ferruginisations et silicifications. Les argiles plastiques du Sparnacien du bassin de Paris, Strasbourg: Université Louis Pasteur Institut de Géologie, Strasbourg, 1981.
[32] L. Pichon, L. Beck, P. Walter, B. Moignard, T. Guillou, Nucl. Instrum. Methods Phys. Res., Sect. B 268 (2010) 2028.
[33] F. Mathis, G. Othmane, O. Vrielynck, H. Calvo del Castillo, G. Chêne, T. Dupuis, D. Strivay, Nucl. Instrum. Methods Phys. Res., Sect. B 268 (2010) 2078.
[34] J.L. Campbell, N.I. Boyd, N. Grassi, P. Bonnick, J.A. Maxwell, Nucl. Instrum. Methods Phys. Res., Sect. B 268 (2010) 3356.